

This article was downloaded by:

On: 26 January 2011

Access details: *Access Details: Free Access*

Publisher *Taylor & Francis*

Informa Ltd Registered in England and Wales Registered Number: 1072954 Registered office: Mortimer House, 37-41 Mortimer Street, London W1T 3JH, UK



## Liquid Crystals

Publication details, including instructions for authors and subscription information:

<http://www.informaworld.com/smpp/title~content=t713926090>

### Theoretical studies of the influence of backflow on the dynamical behaviour of a Fredericks transition of a ferroelectric smectic C\* liquid crystal in the bookshelf geometry

Tomas Carlsson<sup>a</sup>; Noel A. Clark<sup>b</sup>; Zhong Zou<sup>b</sup>

<sup>a</sup> Physics Department, Chalmers University of Technology, Göteborg, Sweden <sup>b</sup> Department of Physics, University of Colorado, Boulder, Colorado, U.S.A.

**To cite this Article** Carlsson, Tomas , Clark, Noel A. and Zou, Zhong(1993) 'Theoretical studies of the influence of backflow on the dynamical behaviour of a Fredericks transition of a ferroelectric smectic C\* liquid crystal in the bookshelf geometry', *Liquid Crystals*, 15: 4, 461 – 477

**To link to this Article:** DOI: 10.1080/02678299308036467

**URL:** <http://dx.doi.org/10.1080/02678299308036467>

PLEASE SCROLL DOWN FOR ARTICLE

Full terms and conditions of use: <http://www.informaworld.com/terms-and-conditions-of-access.pdf>

This article may be used for research, teaching and private study purposes. Any substantial or systematic reproduction, re-distribution, re-selling, loan or sub-licensing, systematic supply or distribution in any form to anyone is expressly forbidden.

The publisher does not give any warranty express or implied or make any representation that the contents will be complete or accurate or up to date. The accuracy of any instructions, formulae and drug doses should be independently verified with primary sources. The publisher shall not be liable for any loss, actions, claims, proceedings, demand or costs or damages whatsoever or howsoever caused arising directly or indirectly in connection with or arising out of the use of this material.

## Theoretical studies of the influence of backflow on the dynamical behaviour of a Fredericks transition of a ferroelectric smectic C\* liquid crystal in the bookshelf geometry

by TOMAS CARLSSON\*

Physics Department, Chalmers University of Technology, S-412 96 Göteborg, Sweden

NOEL A. CLARK and ZHONG ZOU

Department of Physics, University of Colorado, Boulder, Colorado 80309, U.S.A.

(Received 4 January 1993; accepted 5 May 1993)

The elastic–hydrodynamic theory for the ferroelectric smectic C\* phase is reviewed and the governing equations for the dynamical behaviour of a surface stabilized ferroelectric liquid crystalline cell are written down, taking the possibility of macroscopic mass flow in the system into account. The influence of backflow effects on the dynamical cell behaviour and a control parameter, determining whether backflow effects will be of importance or not, is derived. It is shown that when backflow effects are pronounced, the response time of the switching can be considerably decreased. Also, the shape of the c-director and velocity profiles across the cell are shown to be strongly dependent on the presence of backflow.

### 1. Introduction

The director dynamics of the ferroelectric smectic C\* ( $S_C^*$ ) phase have been studied intensively during the past decade. The main reason for this interest is, of course, the discovery that liquid crystals in the  $S_C^*$  phase can be used for developing [1] electro-optical devices. The analysis of all dynamical studies of the  $S_C^*$  phase has up to now been performed with the assumption that no macroscopic flow is coupled to the reorientation of the director. One reason for this neglect is that the proper formulation of the hydrodynamic equations of the  $S_C^*$  phase which is needed in order to incorporate the macroscopic flow into the analysis has become available only recently [2, 3]. However, one knows from the study of nematic liquid crystals that backflow effects [4, 5] play an essential role when analysing the dynamical properties and can practically never be neglected in a complete analysis of the director reorientation of the system. The purpose of this paper is to investigate to what extent backflow effects are also essential for the switching behaviour of a surface stabilized ferroelectric liquid crystal (SSFLC) cell. In the analysis we will apply the recently formulated dynamical theory of  $S_C^*$  liquid crystals [2, 3] in studying the dynamics of an electrically induced Fredericks transition in a SSFLC.

The outline of the paper is as follows: In §2 we define the quantities necessary to describe the system we study, introducing coordinates and notations. We also specify the geometry of the particular Fredericks transition for which we study the influence of backflow on the dynamical behaviour. In §3 we write down the general elastic–hydrodynamic equations governing the dynamical behaviour of the  $S_C^*$  phase. The tilt

\* Author for correspondence

angle dependence of the twenty viscosity coefficients and nine elastic constants, needed by symmetry to describe the system, is described in §4. With the equations written down in §3 as a starting point, in §5 the equations governing the dynamics of the Fredericks transition are derived. As we will only study the initial part of the transition, we also write down the linearized version of these equations. As a reference, in §6 we solve these equations neglecting backflow effects. Finally, in §7, we incorporate backflow into the analysis. Thus, by comparing with the results in the previous section, we are able to show under which circumstances and in which way backflow will influence the dynamical behaviour of the Fredericks transition we have chosen to study.

## 2. A Fredericks transition in a SSFLC—introduction of notation and definition of coordinates

The basic quantities needed to describe a  $S_C^*$  liquid crystal are defined in figure 1. In this work we assume the smectic layers to consist of uniform planes with a fixed orientation, parallel to the  $xy$  plane. The layer normal, thus being parallel to the  $z$  axis, is denoted  $\mathbf{a}$ . Studying an incompressible, dislocation-free medium the layer normal must be subject to the constraint [6]

$$\nabla \times \mathbf{a} = 0, \quad (1)$$

a constraint that is automatically fulfilled within the assumption  $\mathbf{a} = \hat{\mathbf{z}}$ . The average orientation of the molecular long axes, the director, is denoted  $\hat{\mathbf{n}}$ , while the projection of the director into the smectic planes is described by a unit vector  $\hat{\mathbf{c}}$ , commonly denoted the  $c$ -director. In order to describe the orientation of the  $c$ -director we introduce the phase angle  $\phi$ , which is the angle between the  $c$ -director and the  $x$  axis, counting  $\phi$  positive for a rotation around the positive  $z$  axis. Unless the system is very close to the  $S_C^* - S_A^*$  phase transition temperature,  $T_c$ , we can assume the tilt angle  $\theta$ , i.e., the angle between the director and the layer normal, to be fixed [7], only depending on the temperature of the system. We will study only the case  $\theta = \text{constant}$  in this work. The spontaneous polarization  $\mathbf{P}$  of a  $S_C^*$  liquid crystal is confined within the smectic planes and is at right angles [8] to the  $c$ -director. Introducing a unit vector  $\mathbf{b}$  according to

$$\mathbf{b} = \mathbf{a} \times \mathbf{c}, \quad (2)$$

this unit vector will coincide with the polarization vector provided we are studying a (+) compound in the nomenclature of Clark and Lagerwall [9]. Assigning the polarization,  $P_0$ , to be positive for a (+) compound and negative for a (−) compound we thus can write

$$\mathbf{P} = P_0 \mathbf{b}. \quad (3)$$

In figure 2(a) is depicted a SSFLC cell of thickness  $d$  in one of its stable ground states. We assume the  $c$ -director to be in the state  $\phi = 0$  throughout the sample, corresponding to the polarization  $\mathbf{P}$  pointing upwards provided we are studying a (+) compound. By applying an electric field  $\mathbf{E}$  in a direction opposing  $\mathbf{P}$ , i.e.  $\mathbf{E} = -E_0 \mathbf{y}$  where  $E_0$  is the magnitude of the field, one will for a strong enough field induce a Fredericks transition. Assuming strong anchoring at the bounding plates, the polarization will now everywhere except at the boundaries of the cell switch to the downward position and the system will adopt the director profile depicted in figure 2(b).

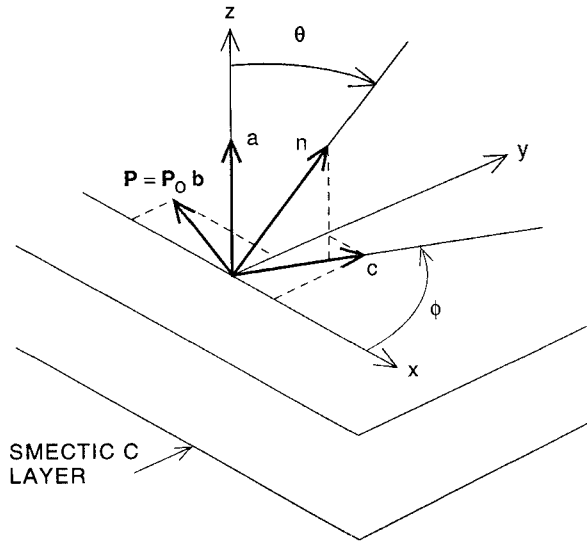


Figure 1. Notation used in the present work. The average molecular direction, the director, is given by a unit vector  $\mathbf{n}$  making an angle  $\theta$  with the layer normal  $\mathbf{a}$ , which is taken to be parallel to the  $z$  axis. The  $c$  director, being a unit vector parallel to the projection of the director into the smectic planes (the  $xy$  plane), is denoted by  $\hat{\mathbf{c}}$  and is described by the phase angle  $\phi$ . The spontaneous polarization  $\mathbf{P}$  is characterized by the unit vector  $\mathbf{b}$  which, if we are studying a (+) compound, is given by the relation  $\mathbf{b} = \mathbf{a} \times \mathbf{c}$ .

Studying the dynamics of this transition, we thus want to calculate the time and space dependence of  $\phi = \phi(y, t)$  for which the initial and boundary conditions are given by

$$\phi(y, 0) = 0, \quad \phi\left(-\frac{d}{2}, t\right) = \phi\left(\frac{d}{2}, t\right) = 0, \tag{4}$$

respectively.

As was pointed out in the introduction we should always expect the transition-between the two states in figure 2 to be accompanied by a macroscopic flow. Due to this flow there will also be a force  $\boldsymbol{\tau} = \tau \hat{\mathbf{x}}$  per unit area exerted on the bounding plates. The velocity vector  $\mathbf{v}$  is, if we consider the system to be incompressible, subject to the constraint

$$\nabla \cdot \mathbf{v} = 0. \tag{5}$$

Furthermore, neglecting the possibility of transportation of material between the smectic layers, the velocity field must fulfil the relation

$$\mathbf{a} \cdot \mathbf{v} = 0, \tag{6}$$

and in the simplest case (neglecting the possibility for the system of developing rolls, i.e. neglecting velocity components in the  $y$  direction) the velocity field will be of the form

$$\mathbf{v} = v(y) \hat{\mathbf{x}}. \tag{7}$$

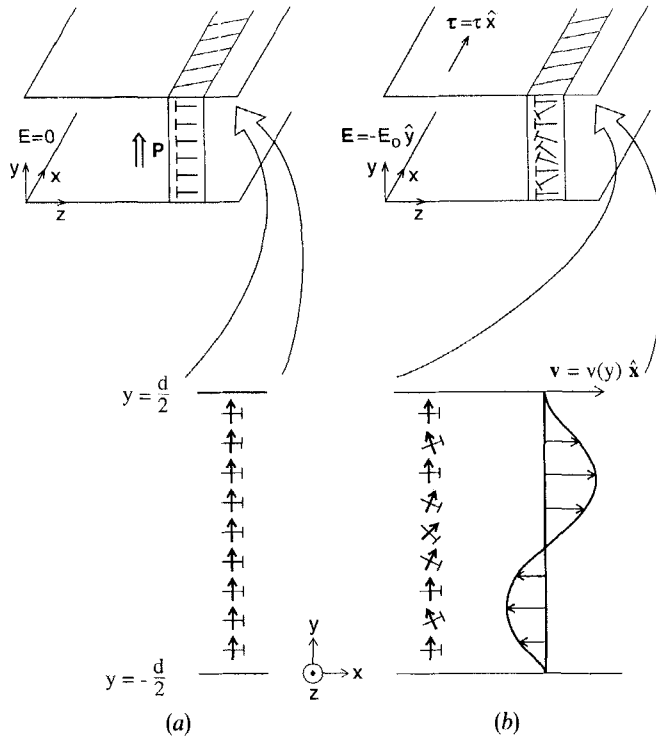


Figure 2. (a) The SSFLC cell in one of its stable states. The  $c$  director is everywhere parallel to the  $x$  axis and the spontaneous polarization  $\mathbf{P}$  is pointing upwards throughout the cell. (b) If a strong enough electric field  $\mathbf{E}$  is applied in a direction opposing the spontaneous polarization, a Fredericks transition will be induced, forcing the polarization to point downwards everywhere except at the boundaries of the cell.

Introducing the usual non-slip condition at the bounding plates, we can assign the following initial and boundary conditions to the velocity field

$$v(y, 0) = 0 \quad v\left(-\frac{d}{2}, t\right) = v\left(\frac{d}{2}, t\right) = 0. \quad (8)$$

The purpose of this paper is now to investigate to what extent the presence of a back-flow of the form discussed above will influence the dynamics of the Fredericks transition depicted in figure 2.

### 3. Summary of the equations governing the elastic–hydrodynamic behaviour of the smectic $C^*$ phase

We now proceed by writing down the equations governing the elastic–hydrodynamic behaviour of the  $S_C^*$  phase. The basic mathematical formulation of these equations has recently been derived by Leslie *et al.* [2, 10], and has been interpreted further and reformulated by Carlsson *et al.* [3]. The governing equations consist of one equation for the balance of linear momentum,

$$\rho \dot{v}_i = F_i + \bar{t}_{ij,j}, \quad (9)$$

and one equation for the balance of angular momentum,

$$\Gamma_i + \varepsilon_{ijk} \tilde{t}_{kj} = 0. \tag{10}$$

In these equations,  $\rho$  is the density of the liquid crystal,  $F_i$  the sum of all external forces and  $\tilde{t}_{ij}$  is the viscous part of the stress tensor. Equation (10) can be interpreted as a balance of torque equation in which the term  $\varepsilon_{ijk} \tilde{t}_{kj}$  is the viscous torque  $\Gamma^v$ , and  $\Gamma_i$  represents the sum of all other torques acting on the system. The viscous part of the stress tensor  $\tilde{t}_{ij}$  is most conveniently expressed as the sum of its symmetrical ( $\tilde{t}_{ij}^s$ ) and antisymmetrical ( $\tilde{t}_{ij}^a$ ) parts

$$\tilde{t}_{ij} = \tilde{t}_{ij}^s + \tilde{t}_{ij}^a. \tag{11}$$

Introducing the following quantities

$$D_{ij} = \frac{1}{2}(v_{i,j} + v_{j,i}), \quad W_{ij} = \frac{1}{2}(v_{i,j} - v_{j,i}), \tag{12}$$

$$D_i^a = D_{ij} a_j \quad D_i^c = D_{ij} c_j, \tag{13}$$

$$A_i = \dot{a}_i - W_{ik} a_k, \quad C_i = \dot{c}_i - W_{ik} c_k, \tag{14}$$

we can write the viscous stress tensor as,

$$\begin{aligned} \tilde{t}_{ij}^s = & \mu_0 D_{ij} + \mu_1 a_p D_p^a a_i a_j + \mu_2 (D_i^a a_j + D_j^a a_i) + \mu_3 c_p D_p^c c_i c_j + \mu_4 (D_i^c c_j + D_j^c c_i) \\ & + \mu_5 c_p D_p^a (a_i c_j + a_j c_i) + \lambda_1 (A_i a_j + A_j a_i) + \lambda_2 (C_i c_j + C_j c_i) + \lambda_3 c_p A_p (a_i c_j + a_j c_i) \\ & + \kappa_1 (D_i^a c_j + D_j^a c_i + D_i^c a_j + D_j^c a_i) + \kappa_2 [a_p D_p^a (a_i c_j + a_j c_i) + 2a_p D_p^c a_i a_j] \\ & + \kappa_3 [c_p D_p^c (a_i c_j + a_j c_i) + 2a_p D_p^c c_i c_j] + \tau_1 (C_i a_j + C_j a_i) + \tau_2 (A_i c_j + A_j c_i) \\ & + 2\tau_3 c_p A_p a_i a_j + 2\tau_4 c_p A_p c_i c_j \end{aligned} \tag{15}$$

$$\begin{aligned} \tilde{t}_{ij}^a = & \lambda_1 (D_j^a a_i - D_i^a a_j) + \lambda_2 (D_j^c c_i - D_i^c c_j) + \lambda_3 c_p D_p^a (a_i c_j - a_j c_i) + \lambda_4 (A_j a_i - A_i a_j) \\ & + \lambda_5 (C_j c_i - C_i c_j) + \lambda_6 c_p A_p (a_i c_j - a_j c_i) + \tau_1 (D_j^a c_i - D_i^a c_j) + \tau_2 (D_j^c a_i - D_i^c a_j) \\ & + \tau_3 a_p D_p^a (a_i c_j - a_j c_i) + \tau_4 c_p D_p^c (a_i c_j - a_j c_i) + \tau_5 (A_j c_i - A_i c_j + C_j a_i - C_i a_j), \end{aligned} \tag{16}$$

where the twenty coefficients  $\mu_i$ ,  $\lambda_i$ ,  $\kappa_i$  and  $\tau_i$  are the viscosity coefficients of the system.

The torques which we will have reason to incorporate in the analysis in this work are, apart from the viscous torque  $\Gamma^v$ , also the elastic torque  $\Gamma^{el}$ , the electric torque  $\Gamma^e$  and the countertorque  $\Gamma^c$ , which is the torque acting on the system in order to keep the layers fixed [3], i.e.

$$\Gamma = \Gamma^{el} + \Gamma^e + \Gamma^c. \tag{17}$$

It is possible to show that when studying a system for which the smectic layers are assumed to be fixed, the  $\theta$ -component of the torque equation (10) is the relevant one to study [3]. Furthermore the symmetry of the system demands [3]

$$\Gamma_\theta^c = 0, \tag{18}$$

where  $\Gamma_\theta^c$  is the  $\theta$ -component of the countertorque.

The  $\theta$ -component of the elastic torque can be calculated as [3, 11].

$$\Gamma_\theta^{el} = \frac{1}{\sin \theta} \left( \frac{\partial g^{el}}{\partial \phi} - \frac{\partial}{\partial x} \frac{\partial g^{el}}{\partial \phi'_x} - \frac{\partial}{\partial y} \frac{\partial g^{el}}{\partial \phi'_y} - \frac{\partial}{\partial z} \frac{\partial g^{el}}{\partial \phi'_z} \right), \tag{19}$$

where  $g^{el}$  is the elastic free energy density which is given by [10, 12]

$$\begin{aligned}
 g^{el} = & \frac{1}{2}A_{12}(\mathbf{b} \cdot \nabla \times \mathbf{c})^2 + \frac{1}{2}A_{21}(\mathbf{c} \cdot \nabla \times \mathbf{b})^2 - A_{11} \left[ \frac{1}{2}(\mathbf{c} \cdot \nabla \times \mathbf{c} - \mathbf{b} \cdot \nabla \times \mathbf{b}) - \delta \right]^2 \\
 & + \frac{1}{2}B_1(\nabla \cdot \mathbf{b})^2 + \frac{1}{2}B_2(\nabla \cdot \mathbf{c})^2 + \frac{1}{2}B_3 \left[ \frac{1}{2}(\mathbf{b} \cdot \nabla \times \mathbf{b} + \mathbf{c} \cdot \nabla \times \mathbf{c}) + q \right]^2 \\
 & + B_{13}(\nabla \cdot \mathbf{b}) \left[ \frac{1}{2} \mathbf{b} \cdot \nabla \times \mathbf{b} + \mathbf{c} \cdot \nabla \times \mathbf{c} \right] \\
 & + C_1(\nabla \cdot \mathbf{c})(\mathbf{b} \cdot \nabla \times \mathbf{c}) + C_2(\nabla \cdot \mathbf{c})(\mathbf{c} \cdot \nabla \times \mathbf{b}).
 \end{aligned} \tag{20}$$

In this expression  $A_i$ ,  $B_i$  and  $C_i$  are the elastic constants of the system,  $q$  is the wave vector of the pitch,  $\delta$  is a material constant related to an inherent tendency of the smectic layers to be non-planar [10], and the unit vectors,  $\mathbf{b}$  and  $\mathbf{c}$  are those already defined by figure 1. In the same manner as above, the electric torque can be calculated as

$$\Gamma_\theta^e = \frac{1}{\sin \theta} \left( \frac{\partial g^e}{\partial \phi} \frac{\partial}{\partial x} \frac{\partial g^e}{\partial \phi'_x} - \frac{\partial}{\partial y} \frac{\partial g^e}{\partial \phi'_y} - \frac{\partial}{\partial z} \frac{\partial g^e}{\partial \phi'_z} \right), \tag{21}$$

where  $g^e$  is the electric free energy density which, including both the ferroelectric and the dielectric coupling, can be written as

$$g^e = \frac{1}{2} \varepsilon_a \varepsilon_0 (\mathbf{n} \cdot \mathbf{E})^2 - \mathbf{P} \cdot \mathbf{E}, \tag{22}$$

where  $\varepsilon_a$  is the dielectric anisotropy of the molecules and  $\varepsilon_0$  is the permittivity of free space. This expression neglects the dielectric biaxiality [13] which is of no concern here as dielectric terms will be discarded anyway in our treatment of the problem.

#### 4. Tilt angle dependence of the viscosity coefficients and the elastic constants

Equations (15), (16) and (20) define twenty viscosity coefficients and nine elastic constants. The temperature dependence of these material parameters does generally have two contributions, one due directly to the tilt angle dependence, in addition to the usual temperature dependence of condensed matter viscosities and elasticities. Studying the system in a not too large temperature interval below the  $S_C^* - S_A^*$  phase transition temperature,  $T_c$ , we can probably, as a fairly good approximation, neglect the second of these two effects. However, as the tilt angle changes dramatically in the temperature interval of interest, we have to take the first of these two effects into account. It can be shown [3] that the symmetry of the system implies that the tilt angle dependence of the viscosity coefficients can be expressed as

$$\left. \begin{aligned}
 \tau_1 = \bar{\tau}_1 \theta, \quad \tau_2 = \bar{\tau}_2 \theta, \quad \tau_3 = \bar{\tau}_3 \theta, \quad \tau_5 = \bar{\tau}_5 \theta, \\
 \kappa_1 = \bar{\kappa}_1 \theta, \quad \kappa_2 = \bar{\kappa}_2 \theta,
 \end{aligned} \right\} \tag{23 a}$$

$$\left. \begin{aligned}
 \lambda_2 = \bar{\lambda}_2 \theta^2, \quad \lambda_3 = \bar{\lambda}_3 \theta^2, \quad \lambda_5 = \bar{\lambda}_5 \theta^2, \quad \lambda_6 = \bar{\lambda}_6 \theta^2, \\
 \mu_4 = \bar{\mu}_4 \theta^2, \quad \mu_5 = \bar{\mu}_5 \theta^2,
 \end{aligned} \right\} \tag{23 b}$$

$$\tau_4 = \bar{\tau}_4 \theta^3, \quad \kappa_3 = \bar{\kappa}_3 \theta^3, \tag{23 c}$$

$$\mu_3 = \bar{\mu}_3 \theta^4, \tag{23 d}$$

where the constants  $\bar{\mu}_i$ ,  $\bar{\lambda}_i$ ,  $\bar{\kappa}_i$  and  $\bar{\tau}_i$  can be assumed to be only weakly temperature dependent. Also the coefficients  $\mu_0$ ,  $\mu_1$ ,  $\mu_2$ ,  $\lambda_1$  and  $\lambda_4$ , which are those remaining in the

$S_A^*$  phase, should be expected to have only a weak temperature dependence. In the same manner we can write the elastic constants as [12]

$$A_{12} = K + \bar{A}_{12}\theta^2, \quad A_{21} = K + \bar{A}_{21}\theta^2, \quad A_{11} = -K + \bar{A}_{11}\theta^2 \quad (24 a)$$

$$B_1 = \bar{B}_1\theta^2, \quad B_2 = \bar{B}_2\theta^2, \quad B_3 = \bar{B}_3\theta^2, \quad (24 b)$$

$$B_{13} = \bar{B}_{13}\theta^3, \quad C_1 = \bar{C}_1\theta, \quad C_2 = \bar{C}_2\theta, \quad (24 c)$$

where again we assume the temperature dependence of  $K$ ,  $\bar{A}_i$ ,  $\bar{B}_i$  and  $\bar{C}_i$  to be weak.

We will employ the scaling properties of the viscosity coefficients and the elastic constants given by equations (23) and (24) throughout this work. The advantage of doing so is that one achieves a better understanding of how the governing equations, and thus the quantities calculated from these, scale with respect to  $\theta$ .

### 5. The dynamic equations governing a SSFLC cell with backflow

In order to study the Fredericks transition depicted in figure 2, one needs to write down the equations governing the two quantities  $\phi(y, t)$  and  $v(y, t)$ . These equations have been derived by us elsewhere [3], with the exception that the ferroelectric torque is not considered in that work. Studying a (+) compound, applying the electric field in a direction opposing the spontaneous polarization vector in the undisturbed cell, i.e.

$$P_x = -P_0 \sin \phi(y, t), \quad P_y = P_0 \cos \phi(y, t), \quad P_z = 0, \quad (25)$$

$$E_x = 0, \quad E_y = -E_0, \quad E_z = 0, \quad (26)$$

the electric energy (22) is, if we neglect the dielectric coupling, given by

$$g^e = P_0 E_0 \cos \phi. \quad (27)$$

From equation (21) we now calculate the ferroelectric torque

$$\Gamma_\theta^e = -\frac{P_0 E_0}{\sin \theta} \sin \phi. \quad (28)$$

Assuming we are studying the system sufficiently close to  $T_c$ , we can employ the approximation  $\sin \theta \approx \theta$ . This approximation will be used in all calculations throughout this paper. As a 'decent' approximation we can also assume that the spontaneous polarization is proportional to the tilt [14], i.e. we introduce a weakly temperature dependent quantity  $\bar{P}$  according to

$$P_0 = \bar{P}\theta. \quad (29)$$

We thus can write the ferroelectric torque (28) as

$$\Gamma_\theta^e = -\bar{P}E_0 \sin \phi. \quad (30)$$

Substituting the ansatz

$$c_x = \cos \phi(y, t), \quad c_y = \sin \phi(y, t), \quad c_z = 0, \quad (31)$$

$$v_x = v(y, t), \quad v_y = 0, \quad v_z = 0, \quad (32)$$

into equations (9)–(16) one can now derive the governing equations of the system. Following [3], and adding the ferroelectric torque (30) to the result of that paper, one



finally derives the following governing equations of the dynamic behaviour of the SSFLC cell,

$$2(\bar{\tau}_5 + \bar{\lambda}_5 \theta^2) \dot{\phi} \theta + [\bar{\tau}_5 + \bar{\lambda}_5 \theta^2 + (\bar{\tau}_2 + \bar{\lambda}_2 \theta^2)(\cos^2 \phi - \sin^2 \phi)] \theta v', \\ - [(\bar{B}_1 \sin^2 \phi + \bar{B}_2 \cos^2 \phi) \phi''_{yy} + \frac{1}{2}(\bar{B}_1 - \bar{B}_2) \sin 2\phi \phi'^2] \theta - \bar{P} E_0 \sin \phi = 0, \quad (33)$$

$$\frac{d}{dy} \left[ \frac{1}{2} \{ \mu_0 + [\bar{\mu}_4 + \bar{\lambda}_5 + 2\bar{\lambda}_2 (\cos^2 \phi - \sin^2 \phi)] \theta^2 + 2\bar{\mu}_3 \sin^2 \phi \cos^2 \phi \theta^4 \} v', \right. \\ \left. + \dot{\phi} [\bar{\lambda}_5 + \bar{\lambda}_2 (\cos^2 \phi - \sin^2 \phi)] \theta^2 \right]. \quad (34)$$

When analysing the Fredericks transition in which we are interested, these equations shall be solved with the boundary conditions

$$\phi \left( -\frac{d}{2}, t \right) = \phi \left( \frac{d}{2}, t \right) = 0, \quad (35)$$

$$v \left( -\frac{d}{2}, t \right) = v \left( \frac{d}{2}, t \right) = 0. \quad (36)$$

The form of the boundary conditions (35) implies that we are studying a system for which the surfaces do not switch in the transition.

The structure of equations (33) and (34) implies that, if one wants to calculate  $\phi(y, t)$  and  $v(y, t)$  for switching for which  $\phi$  is large, or where different boundary conditions for  $\phi$  are assumed to apply on the two bounding glass plates, one has to perform the calculation numerically. Such numerical solutions of these equations in some different cases are underway and will be published in future work [15]. Here, we will however be content to study only the start of the switching, and thus it is sufficient to study the linearized version of equations (33) and (34). Doing so we will be able to discuss some general feature of the dynamics of the transition and also make some general statements regarding the influence of backflow. Assuming  $\phi$  to be small, and neglecting terms of second power and higher in  $\phi$ , equations (33) and (34) can be transformed into

$$\frac{\bar{B}_2 \theta}{\bar{P} E_0} \phi'' + \phi = \frac{2(\bar{\tau}_5 + \bar{\lambda}_5 \theta^2) \theta}{\bar{P} E_0} \dot{\phi} + \frac{[\bar{\tau}_2 + \bar{\tau}_5 + (\bar{\lambda}_2 + \bar{\lambda}_5) \theta^2] \theta}{\bar{P} E_0} v', \quad (37)$$

$$\frac{d}{dy} \left[ \frac{1}{2} \{ \mu_0 + (\bar{\mu}_4 + \bar{\lambda}_5 + 2\bar{\lambda}_2) \theta^2 \} v' + (\bar{\lambda}_2 + \bar{\lambda}_5) \theta^2 \dot{\phi} \right] = 0. \quad (38)$$

In the next section we will show that the critical field  $E_c$  for which the Fredericks transition is induced is given by

$$E_c = \frac{\bar{B}_2 \pi^2 \theta}{\bar{P} d^2}. \quad (39)$$

By introducing the reduced field  $\varepsilon$ ,

$$\varepsilon = \frac{E_0}{E_c} = \frac{\bar{P} d^2 E_0}{\bar{B}_2 \pi^2 \theta}, \quad (40)$$

and also by making the following definitions,

$$\alpha = \frac{\bar{\tau}_2 + \bar{\tau}_5 + (\bar{\lambda}_2 + \bar{\lambda}_5) \theta^2}{2(\bar{\tau}_5 + \bar{\lambda}_5 \theta^2)}, \quad \beta = \frac{2(\bar{\tau}_5 + \bar{\lambda}_5 \theta^2) \theta}{\bar{P} E_0}, \quad (41 a)$$

$$a = \frac{1}{2} \{ \mu_0 + (\bar{\mu}_4 + \bar{\lambda}_5 + 2\bar{\lambda}_2) \theta^2 \}, \quad b = (\bar{\lambda}_2 + \bar{\lambda}_5) \theta^2, \quad (41 b)$$

equations (37) and (38) can be written as

$$\frac{d^2}{\pi^2 \varepsilon} \phi'' + \phi = \beta \dot{\phi} + \beta \alpha v', \quad (42)$$

$$\frac{d}{dy} [av' + b\dot{\phi}] = 0. \quad (43)$$

Equations (42) and (43), together with the boundary conditions (35) and (36), are the equations which we will solve.

### 6. Study of the threshold neglecting backflow

In this section we study the transition, assuming that backflow effects are not induced by the reorientation of the director. To do so we neglect the term  $\beta \alpha v'$  in equation (42), and look for a solution, fulfilling the boundary condition (35), of the equation thus obtained,

$$\frac{d^2}{\pi^2 \varepsilon} \phi'' + \phi = \beta \dot{\phi}. \quad (44)$$

In this equation  $\varepsilon$  is the reduced field defined by equation (40),  $d$  is the sample thickness and  $\beta$  is the constant with the dimension of time defined by equation (41 a). Generally, the solution of equation (44) can be written as a Fourier series. Studying the transition just above the threshold, it is enough to retain only the slowest varying term of this series and we thus make the following ansatz for the solution,

$$\phi = \phi_0 \cos \frac{\pi y}{d} \exp\left(\frac{t}{t_0}\right). \quad (45)$$

Substituting equation (45) into equation (44), we calculate the response time  $t_0$  of the transition,

$$t_0 = \beta \frac{\varepsilon}{\varepsilon - 1}. \quad (46)$$

From equation (46) we see that  $\varepsilon < 1$  implies that  $t_0 < 0$ , and thus a fluctuation  $\phi = \phi_0 \cos(\pi y/d)$  of the c-director decreases exponentially back to the undisturbed configuration. On the other hand,  $\varepsilon > 1$  implies that  $t_0 > 0$ , and the corresponding fluctuations will be amplified by the electric field inducing the Fredericks transition. Thus we have proven that the definition (39) represents the critical field  $E_c$  for which the transition will occur. Substituting equations (40) and (41 a) into equation (46) we can write the response time  $t_0$  as

$$t_0 = \frac{\bar{t}_0}{\varepsilon - 1}, \quad (47)$$

where the constant

$$\bar{t}_0 = \frac{2(\bar{\tau}_5 + \bar{\lambda}_5 \theta^2) d^2}{\bar{B}_2 \pi^2}, \quad (48)$$

represents a typical time scale of the system. From equation (47) we notice that when the field just exceeds the critical one ( $\varepsilon \gtrsim 1$ ), the transition is infinitely slow. By this reason we do not expect backflow effects to influence the expression of the critical field  $E_c$ . However, for large electric fields ( $\varepsilon \gg 1$ ), we show in the next section that not only the

response time  $t_0$ , but also the profile (45) of the c-director will be influenced by backflow effects.

### 7. Influence of backflow

In the previous section we calculated the response time (equations (46)–(48)) of the Fredericks transition, and the c-director profile (equation (45)) as it appears at the start of the switching, assuming that the backflow effects are negligible. We will now investigate to what extent these results are modified when backflow is taken into account in the calculations. The approach we use is similar to that by Pieranski *et al.* [4, 5], when analysing the influence of backflow for a similar problem in nematic liquid crystals.

#### 7.1. Solving the equations

In order to study the dynamical behaviour of the Fredericks transition we shall solve equations (42) and (43) together with the boundary conditions (35) and (36). It is easily seen from equation (43) that the ansatz for the c-director  $\phi = \phi_0(t) \cos(\pi y/d)$  implies a velocity profile  $v = v_0(t) \sin(\pi y/d)$ . However, this solution does not fulfil the non-slip conditions (36) on bounding plates. In order to fulfil the boundary conditions (35) and (36) for both  $\phi(y, t)$  and  $v(y, t)$ , we thus have to make a more complex ansatz [4, 5]

$$\phi = \phi_0 \left( \cos qy - \cos \frac{qd}{2} \right) \exp \left( \frac{t}{t_b} \right), \quad (49)$$

$$v = v_0 \left( \sin qy - \frac{2y}{d} \sin \frac{qd}{2} \right) \exp \left( \frac{t}{t_b} \right). \quad (50)$$

We see that this solution does not follow the quasistatic state, and the wave vector of the distortion  $q$  and the response time  $t_b$  are, due to the backflow, functions of the magnitude of the applied electric field  $\varepsilon$ . Substituting equations (49) and (50) into equations (42) and (43), one derives the following three relations for the four quantities  $q$ ,  $t_b$ ,  $f_0$  and  $v_0$ ,

$$-\frac{d^2}{\pi^2 \varepsilon} q^2 \phi_0 + \phi_0 = \frac{\beta \phi_0}{t_b} + \alpha \beta v_0 q, \quad (51)$$

$$\phi_0 \cos \frac{qd}{2} = \beta \phi_0 \cos \frac{qd}{2} + \frac{2\alpha \beta v_0}{d} \sin \frac{qd}{2}, \quad (52)$$

$$\phi_0 = -\frac{aqt_b}{b} v_0. \quad (53)$$

By introducing the definitions

$$A = \frac{b\alpha}{a}, \quad X = \frac{qd}{2}, \quad (54)$$

the solution of equations (51)–(53) can be written as

$$\varepsilon = \frac{4X^2 \tan X - (X/A)}{\pi^2 \tan X - X}, \quad (55)$$

$$t_b = \beta \left( 1 - \frac{A \tan X}{X} \right). \quad (56)$$

Equations (55) and (56) shall be interpreted in the following way. For a given set of viscosity coefficients, the parameter  $A$ , which is defined by equations (41) and (54), adopts a specific value. The viscosity coefficients can be shown to fulfil certain inequalities [3], and from these it can be proven that the parameter  $A$  must always be positive. Furthermore it can be seen from equations (55) and (56) that, if the value of  $A$  exceeds unity, the solution of these equations will exhibit discontinuities which correspond to a behaviour of the system which probably is unphysical. In their papers [4, 5], Pieranski *et al.*, claim that for a nematic liquid crystal, the constant corresponding to  $A$  cannot exceed unity. We cannot formally prove that this must be the case also for the system we study, but this seems probable. Thus we assume

$$0 < A < 1 \quad (57)$$

to be valid in order to avoid discussing unphysical solutions of equations (55)–(56).

For a given value of  $A$ , equation (55) gives a relation between the reduced electric field  $\varepsilon$  and the wave vector of the distortion, which is determined by the quantity  $X$ . When  $\varepsilon$  is varied between unity and infinity,  $X$  varies between  $\pi/2$  and 4.49. We now introduce the dimensionless parameter  $\eta$  by either of the relations

$$q = \eta \frac{\pi}{d}, \quad X = \eta \frac{\pi}{2}. \quad (58)$$

Thus  $\eta$  measures the deviation of the wave vector  $q$  of the distortion from its quasistatic value  $\pi/d$ . When  $X$  varies between the two limits given above,  $\eta$  varies between unity and 2.85.

Once  $X$  is calculated for a given value of  $\varepsilon$  by the use of equation (55), the response time of the transition,  $t_b$ , is given by equation (56). However, we will rather be interested in the ratio between the response time calculated with ( $t_b$ ) and without ( $t_0$ ) backflow effects being taken into account, and from equations (46) and (56) we can write

$$\frac{t_b}{t_0} = \frac{\varepsilon - 1}{\varepsilon} \left( 1 - \frac{A \tan X}{X} \right). \quad (59)$$

## 7.2. Numerical results

In figure 3 is depicted how the wave vector of the distortion  $q$  varies with the applied reduced electric field  $\varepsilon$  for four different values of the parameter  $A$ . We prefer to show the value of  $\eta$ , which is the ratio of  $q$  when backflow effects are taken into account and its quasistatic value  $\pi/d$ . We notice from the figure that when  $A$  is small,  $\eta$  is close to unity and backflow effects are negligible. When  $A$  becomes larger and approaches unity, backflow effects become pronounced and the wave vector of the distortion increases. The ratio of the response times calculated with and without backflow (equation (59)) is depicted in figure 4, using the same sequence of  $A$  as above. Again we notice how backflow effects become pronounced as the value of the parameter  $A$  increases. As is seen from the figure, backflow effects speed up the response time of the transition considerably if  $A$  is large enough.

As was discussed above, for a certain combination of the parameter  $A$  and the reduced field  $\varepsilon$ , the c-director (equation (49)) and the velocity (equation (50)) profiles of the distortion can be characterized by the parameter  $\eta$ , which fulfils the relation

$$1 < \eta < 2.85. \quad (60)$$

In figure 5 we show how the envelopes of the profiles  $\phi(y, t)$  and  $v(y, t)$  change when  $\eta$  is varied between these two limits. We notice that for a large value of  $\eta$ , when backflow

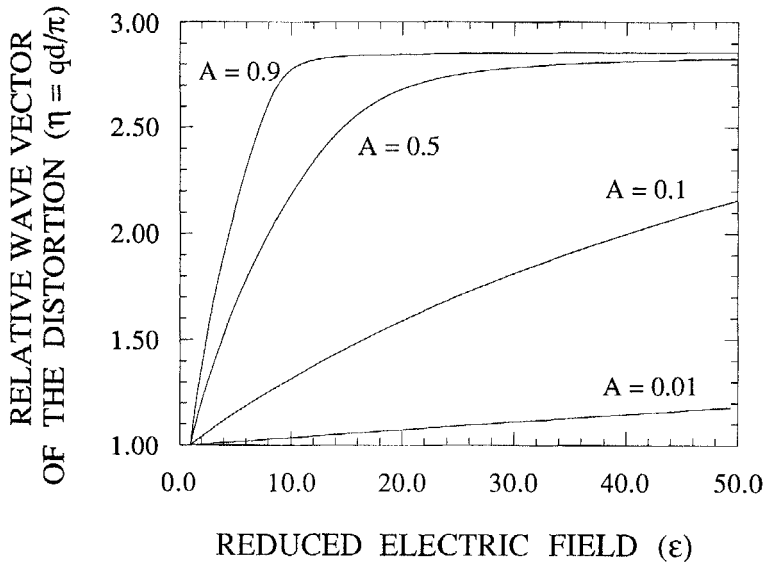


Figure 3. The ratio,  $\eta$ , of the wave vector of the distortion  $q$ , calculated with and without backflow effects being taken into account. The figure depicts how  $\eta$  varies with the applied reduced electric field  $\epsilon$  for four different values of the parameter  $A$ .

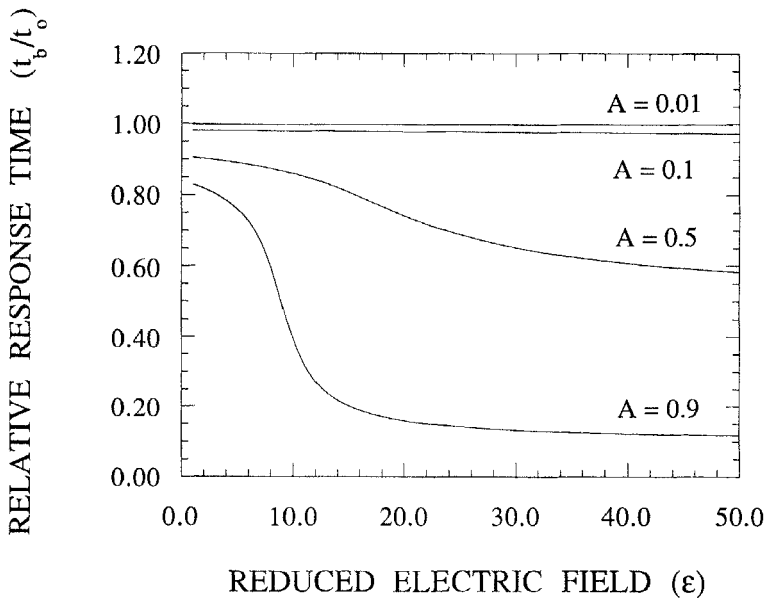


Figure 4. The ratio  $t_b/t_0$  of the response times calculated with and without backflow effects being taken into account. The figure depicts how  $t_b/t_0$  varies with applied reduced electric field  $\epsilon$  for four different values of the parameter  $A$ .

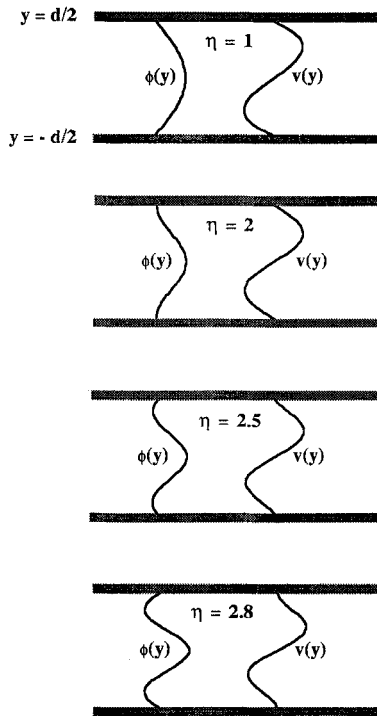


Figure 5. The envelopes of the c-director and velocity profiles as functions of  $\eta$ .

effects are pronounced, the switching of the c-director starts in the ‘wrong’ direction close to the boundaries of the glass plates.

7.3. Formations of  $2\pi$  disclination walls as a consequence of backflow

From the discussion in §7.2 it is clear that backflow can cause the switching of the c-director in some cases to start in different directions in different parts of the sample. The condition for this to happen is that the derivative  $d\phi/dz$  shall be negative at the lower plate, i.e.

$$\left. \frac{d\phi}{dy} \right|_{y=-d/2} < 0, \tag{61}$$

which, with the ansatz (49) for  $\phi(y)$ , is equivalent to the condition  $\eta > 2$ . Thus, whenever the combination of the material parameter  $A$  and the reduced electric field  $\varepsilon$  is such that the calculated  $\eta$  in figure 3 exceeds two, there is a possibility of the formation of two  $2\pi$  walls close to the bounding plates.

In figure 6 is a sequence of the time evolution of the envelopes  $\phi(y, t)$  and  $v(y, t)$  which have been calculated by solving the governing equations (33) and (34) numerically [15]. The choice of the parameter  $A$  is  $A = 0.5$  and the reduced field is put equal to  $\varepsilon = 5, 40$  and  $100$ , respectively. From figure 3 it is seen that, for  $A = 0.5$ , the limiting value of the reduced field for which the switching close to the bounding plates goes in the opposite direction to that in the bulk is close to  $\varepsilon = 8$ . In the upper part of figure 6 we have chosen  $\varepsilon = 5$ , and it can be seen that the switching proceeds homogeneously in the whole sample. Increasing the field to  $\varepsilon = 40$  (middle part of

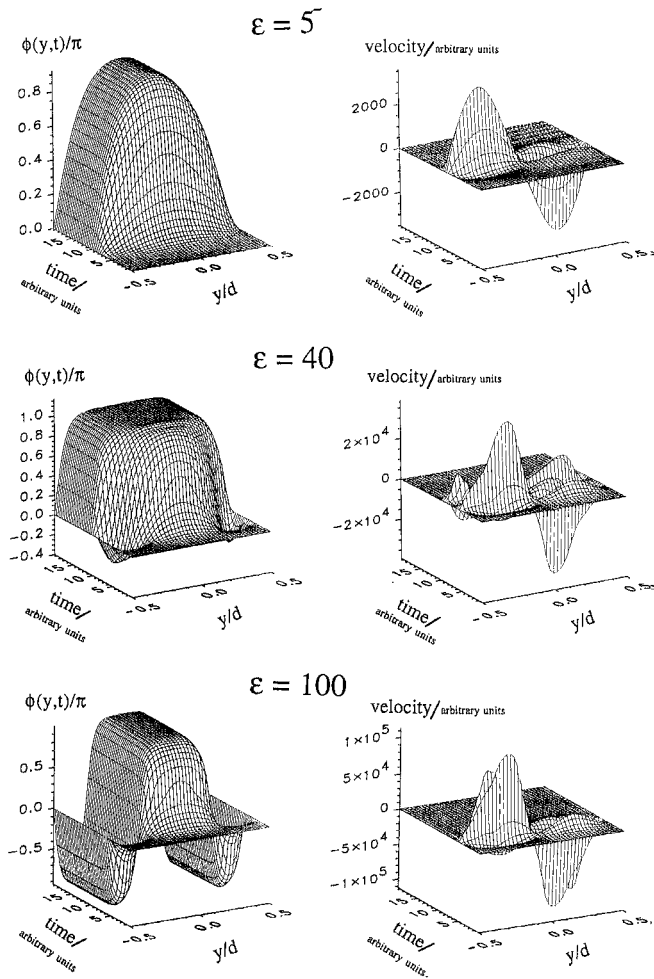


Figure 6. Time evolution (obtained by numerical solution [15] of the governing equations) of the envelopes  $\phi(y, t)$  and  $v(y, t)$  for three different reduced electric fields  $\epsilon$ . When  $\epsilon < 8$ , the switching of the  $c$ -director is homogeneous throughout the sample (upper part). When  $\epsilon > 8$ , backflow effects cause the switching to start in the 'wrong' direction close to the bounding plates. Elasticity will however drive the system to a final state, which is homogeneous if  $\epsilon$  is not too large (middle part). Increasing  $\epsilon$  enough, the ferroelectric torque will dominate over the elastic torque, and the final state will exhibit two  $2\pi$  walls close to the bounding plates (lower part). The parameter  $A$  is chosen to be  $A = 0.5$  in the calculation.

figure), one sees how the switching close to the boundaries starts in the 'wrong' direction. However, the elastic torque will eventually overcome the ferroelectric torque and the final state will still be homogeneous. If the electric field is large enough, as in the lower part of the figure ( $\epsilon = 100$ ), the ferroelectric torque dominates over the elastic torque and the final configuration of the system exhibits two  $2\pi$  walls close to the bounding plates. We thus conclude that trying to decrease the response time by increasing the field will ultimately, due to backflow effects, create two  $2\pi$  disclinations in the sample, destroying the homogeneously ordered final state which we might be trying to achieve.

#### 7.4. The force on the bounding plates

When the cell is switching, a force  $\tau = \tau \hat{x}$  per unit area is exerted on the bounding plates. This force can be calculated from equation (43). By integrating this equation, the constant of integration will correspond to  $\tau$  and one obtains

$$\tau = av' + b\dot{\phi}. \quad (62)$$

Substituting equations (49) and (50) into equation (62), and employing the relation (53) one derives

$$\tau = a \left( q \cos \frac{qd}{2} - \frac{2}{d} \sin \frac{qd}{2} \right) v_0 \exp(t/t_b) = \quad (63)$$

$$= \frac{b}{qt_b} \left( \frac{2}{d} \sin \frac{qd}{2} - q \cos \frac{qd}{2} \right) \phi_0 \exp(t/t_b). \quad (64)$$

Thus we observe that switching the cell in an oscillatory manner, due to an alternating electric field, induces an oscillating force on the bounding plates. This force is probably the force that is driving the electromechanical coupling in SSFLCs which has been observed by Eber *et al.* [16].

## 8. Discussion

By employing the recently developed elastic–hydrodynamic theory of the  $S_C^*$  phase [2, 3, 10], in this work we have shown to what extent backflow effects influence the switching of a SSFLC in one case, i.e. the Fredericks transition in the geometry depicted in figure 2. Among the 20 viscosity coefficients and 9 elastic constants for a complete description of the system, only six viscosities ( $\tau_2, \tau_5, \lambda_2, \lambda_5, \mu_0$  and  $\mu_4$ ) and one elastic constant ( $B_2$ ) enter the governing equations (42) and (43) of the situation analysed in this work. These material parameters must fulfil [3, 5] the scaling relations given by equations (23) and (24). Employing this scaling, we introduce the constants  $\bar{\tau}_2, \bar{\tau}_5, \bar{\lambda}_2, \bar{\lambda}_5, \bar{\mu}_0, \bar{\mu}_4$  and  $\bar{B}_2$ , the temperature dependence of which can be assumed to be negligible to a fairly high degree of accuracy. Within the model which we are working, the governing equations and consequently all results are explicitly expressed using this scaling. Thus, the temperature dependence of the results implicitly enters through the temperature dependence of  $\theta$ .

Both the viscosity coefficients [3] and the elastic constant [5] must fulfil certain inequalities. Those relevant for this work are

$$\bar{\lambda}_5 > 0, \quad \bar{\tau}_5 > 0, \quad \bar{\lambda}_5 > \bar{\tau}_5, \quad \mu_0 > 0, \quad (65)$$

$$\bar{B}_2 > 0. \quad (66)$$

Furthermore, one can prove that, providing we are studying a (+) compound ( $\bar{P} > 0$ ), the constants  $a$  and  $\beta$ , which are defined by equation (48), must also be positive,

$$a > 0, \quad \beta > 0. \quad (67)$$

For the Fredericks transition we study, we have been able to recast the governing equations in such a way that only one parameter ( $A = b\alpha/a$ , c.f. equations (41)) governs the behaviour of the transition. This parameter depends only on the values of the viscosity coefficients and can be shown [3] to be positive. As was mentioned before, we cannot prove that  $A$  is always smaller than unity, but as the opposite case produces



unphysical solutions of the governing equations, we have only considered the case  $0 < A < 1$  in this work, leaving the formal proof of this relation for future work. For a small  $A$ , backflow effects are negligible, while they become important as  $A$  approaches unity. That this is the case can be understood qualitatively in the following way. The constant  $A$  is proportional to the ratio  $a/b$ . It can be shown [3], that the constants  $a$  and  $b$  are proportional to the effective shearing viscosity and the rotational viscosity, respectively. A small value of  $b/a$  corresponds to the case when the shearing viscosity is comparatively large and a macroscopic shear flow in the system is rapidly damped. Thus backflow effects will not be of importance in this case. If, on the other hand,  $b/a$  is large, the shearing viscosity is small and a macroscopic flow is more easily developed in the system. The constant  $A$  is also proportional to  $\alpha$ . From a mathematical point of view, it is obvious that whenever  $\alpha$  is small, the influence of the term proportional to  $v'$  in the switching equation (42) decreases, and thus the influence of backflow becomes less pronounced. We can understand the physical reason for this behaviour by examining equation (37), which can be interpreted as a balance of torque equation. The two terms on the right-hand side are proportional to the rotational and the shearing torques, respectively. Thus, the constant  $\alpha$  (equation (41 a)) represents the ratio of the coupling constants of the shearing torque (for  $\phi = 0$ ) and the rotational torque. If this ratio is large, it is comparatively easy to induce a shear in the system and backflow effects should be expected to be pronounced. If  $\alpha$  is small, on the other hand, backflow effects should be negligible.

Figures 3–6 show how backflow effects influence the switching of the cell and represent the main results of this paper. Figure 3 clearly shows how backflow effects depend on  $A$  as well as  $\varepsilon$ . Furthermore, one notices that the more important the backflow effects become, the larger is the wave vector of the distortion  $q = \pi\eta/d$ , as shown in figure 5 which depicts how the envelopes of the profiles  $\phi(y, t)$  and  $v(y, t)$  change as functions of  $\eta$ . We should also remember that in this figure, the graphs only represent the normalized shapes of  $\phi(y, t)$  and  $v(y, t)$ , and are not related to the amplitudes  $\phi_0$  and  $v_0$ . As is seen from equation (53),  $v_0 \sim b/a\phi_0$  and as discussed above, when  $b/a$  is small, backflow effects are negligible and accordingly the amplitude  $v_0$  of the velocity profile approaches zero. One interesting effect of backflow can be noticed in figures 5 and 6. When the backflow effects are pronounced, the switching close to the bounding plates starts in the ‘wrong’ direction. This will, for strong enough electric fields, lead to the formation of disclinations in the sample, destroying the homogeneously ordered final state we might have expected. Nevertheless, it is clear from figure 4, that the backflow effects, if these are large enough, will speed up the switching considerably.

Since we have solved only the linearized equations (42) and (43), the results of this paper (with the exception of figure 6) apply only to the start of the switching. Nevertheless, we have been able to calculate the value of the typical response time of the transition and to characterize the crucial parameter ( $A$ ), which determines to what extent backflow effects influence the switching. If we want to study the full switching of the system, or the case when different boundary conditions apply on the bounding plates, we are instead forced to solve equations (33) and (34). These equations must, however, be solved numerically. One result of such studies is shown in figure 6 and a full account of these calculations will be published in the future [15]. However, by rewriting equations (33) and (34) into a form similar to that of equations (42) and (43), we can still derive an expression of the crucial parameter determining whether backflow effects should be expected to be important or not. This parameter is the parameter

corresponding to  $A$ , but will now depend on the orientation of the c-director, i.e. we shall study the parameter  $A(\phi)$  given by

$$A(\phi) = \frac{[\bar{\lambda}_5 + \bar{\lambda}_2(\cos^2 \phi - \sin^2 \phi)][\bar{\tau}_5 + \bar{\lambda}_5\theta^2 + (\bar{\tau}_2 + \bar{\lambda}_2\theta^2)(\cos^2 \phi - \sin^2 \phi)]\theta^2}{(\bar{\tau}_5 + \bar{\lambda}_5\theta^2)\{\mu_0 + [\bar{\mu}_4 + \bar{\lambda}_5 + 2\bar{\lambda}_2(\cos^2 \phi - \sin^2 \phi)]\theta^2 + 2\bar{\mu}_3 \sin^2 \phi \cos^2 \phi \theta^4\}} \quad (68)$$

The value of this parameter will change during the switching and also be different in different parts of the cell. Anyhow, as a rule of thumb, whenever we find  $A(\phi)$  to be close to unity, we shall expect backflow to occur in the corresponding part of the cell. It is also obvious that if backflow occurs in some part of the cell, flow will be induced in the neighbouring parts of the cell due to viscous forces.

In conclusion, in this paper we have shown that backflow effects should be expected to influence the switching behaviour of a SSFLC cell in most cases. We have been able to identify the parameter,  $A$  (equation (54)), or in the more general case  $A(\phi)$  (equation (68)), the value of which determines whether backflow effects will be of importance or not. However, as rather little experimental information about the values of the viscosity coefficients of the  $S_C^*$  phase exists today, we cannot make any statements regarding experimental values of  $A$ . Thus, the experimental determination of these coefficients must be considered as one of the urgent tasks to be undertaken in the current research concerning the dynamical behaviour of the  $S_C^*$  phase.

### References

- [1] CLARK, N. A., and LAGERWALL, S. T., 1980, *Appl. Phys. Lett.*, **36**, 899.
- [2] LESLIE, F. M., STEWART, I. W., and NAKAGAWA, M., 1991, *Molec. Crystals liq. Crystals*, **198**, 443.
- [3] CARLSSON, T., LESLIE, F. M., and CLARK, N. A., *Phys. Rev. A* (submitted).
- [4] BROCHARD, F., PIERANSKI, P., and GUYON, E., 1972, *Phys. Rev. Lett.*, **28**, 1681.
- [5] PIERANSKI, P., BROCHARD, F., and GUYON, E., 1973, *J. Phys., Paris*, **34**, 35.
- [6] OSEEN, C. W., 1933, *Trans. Faraday Soc.*, **29**, 883.
- [7] CARLSSON, T., and DAHL, I., 1983, *Molec. Crystals liq. Crystals*, **95**, 373.
- [8] MEYER, R. B., LIEBERT, L., STRZELECKI, L., and KELLER, P. J., 1975, *J. Phys. Lett., Paris*, **36**, L69.
- [9] CLARK, N. A., and LAGERWALL, S. T., 1984, *Ferroelectrics*, **59**, 25.
- [10] CARLSSON, T., STEWART, I. W., and LESLIE, F. M., 1992, *J. Phys. A*, **25**, 2371.
- [11] CARLSSON, T., 1986, *Phys. Rev. A*, **34**, 3393.
- [12] CARLSSON, T., STEWART, I. W., and LESLIE, F. M., 1991, *Liq. Crystals*, **9**, 661.
- [13] JONES, J. C., RAYNES, E. P., TOWLER, M. J., and SAMBLES, J. R., 1990, *Molec. crystals liq. Crystals Lett.*, **7**, 91.
- [14] DUMRONGRATTANA, S., and HUANG, C. C., 1986, *Phys. Rev. Lett.*, **56**, 464.
- [15] ZOU, Z., CLARK, N. A., and CARLSSON, T. (to be published).
- [16] EBER, N., KOMITOV, L., LAGERWALL, S. T., MATUSZCZYK, M., SKARP, K., and STEBLER, B., 1992, *Ferroelectrics*, **129**, 19.